An extended coupling model description of the evolution of dynamics with time in supercooled liquids and ionic conductors

2003 J. Phys.: Condens. Matter 15 S1107

(http://iopscience.iop.org/0953-8984/15/11/332)

INSTITUTE OF PHYSICS PUBLISHING JOURNAL OF PHYSICS: CONDENSED MATTER

J. Phys.: Condens. Matter **15** (2003) S1107–S1125 PII: S0953-8984(03)57915-2

An extended coupling model description of the evolution of dynamics with time in supercooled liquids and ionic conductors

K L Ngai

Naval Research Laboratory, Washington, DC 20375-5320, USA

E-mail: ngai@estd.nrl.navy.mil

Received 27 September 2002
Published 10 March 2003
Online at stacks.iop.org/JPhysCM/15/S1107

Abstract

In the past the coupling model (CM) was focused on the dynamics at long times, when all relaxing units of an interacting system participate in the terminal, cooperative Kohlrausch relaxation. No attention was paid to the dynamics at short times when all the relaxing units are caged, nor to intermediate times when an increasing number of them are no longer caged. We now extend the CM to also address the dynamics in these earlier time regimes. The crux of the extended CM is the quantitatively determinable independent relaxation time, from which the characteristics of the dynamics in the short-time and intermediate-time regimes can be deduced. This description of the evolution of the dynamics by the extended CM is supported by broadband dielectric relaxation spectra of two archetypal systems, the glassy/molten ionic conductors and supercooled liquids. In supercooled liquids, the 'universal' Johari–Goldstein β-relaxation provides evidence for the physical reality of the independent relaxation of the extended CM.

(Some figures in this article are in colour only in the electronic version)

1. Introduction

The dynamics of several classes of cooperatively relaxing systems are active areas of research. These include the molecular dynamics of glass-forming supercooled liquids of all kinds [1–14], the ion dynamics in glassy or molten ionic conductors [15–25] and the colloidal particle suspensions [26, 27]. Not only are the dynamics of a material in any class of interest in their own right, but also of broader interest is the existence of common features in the dynamics of different classes [28]. The latter suggests that some fundamental physics governs the dynamics of all cooperatively relaxing systems, and any theoretical description should be general enough to be applicable to all classes. Due to recent developments in experimental capabilities, the dynamics can now be measured over much wider time/frequency ranges. It is advantageous to

have a theoretical description of the dynamics that covers continuously from short times, when the relaxing units are caged and only local motions are possible, to long times, when they are engaged in cooperative motion, eventually giving rise to flow, diffusion or conductivity. The validity of the description should not be confined to any specific time or temperature range. In the course of time, several general and often anomalous properties of the long-time cooperative dynamics have been found, requiring a theoretical explanation. Fulfilling all these requirements would need a Herculean theoretical effort, not achieved so far. Most efforts are confined to addressing only some properties in certain dynamic regimes. For example, the idealized mode coupling theory is mainly confined to describing the caged dynamics of colloidal particles and glass-forming liquids at temperatures above a critical temperature, T_c, high above the glass transition temperature, T_g [29]. Based on density considerations, it does not apply to the dynamics of ions in glassy ionic conductors or molten ionic conductors at temperatures where the ion dynamics are decoupled from the structural relaxation. The coupling model (CM) of the present author [30–34], in previous publications, was restricted to addressing the long-time cooperative dynamics and the transport coefficients. It has general applicability to all cooperatively relaxing systems and is successful in rationalizing or explaining their general and often anomalous properties [28, 34]. Nevertheless, no effort was made to describe the short-time dynamics that precede the cooperative dynamics, a deficiency which invited legitimate criticisms [35, 36]. The objective of the present work is to fill this void of the CM, by offering a description of the short-time dynamics, and to arrive at an extended CM appropriate for all times. Experimental spectra of materials in several classes of cooperatively relaxing systems are used to identify the general features of the short-time dynamics, and to assess the extended CM.

2. The coupling model extended

We shall first clarify that the CM in most previous applications was confined to the consideration of only the long-time cooperative dynamics based on the scenario that all relaxing units are no longer caged. The key concept therein is the independent relaxation, which is slowed down by the mutual interactions between the relaxing units starting at a temperature independent time, t_c, with its magnitude determined by the strength of the interaction [30–34]. The independent relaxation time, τ_0, can be calculated from the experimentally observed cooperative relaxation time, τ. After that we extend the CM to address the dynamics at shorter times. The independent relaxation time, τ_0, now plays a pivotal role in delineating the short-time, the intermediate-time and the long-time regimes. From the physical meaning of τ_0, we deduce the nature of the dynamics in the short-time and intermediate-time regimes. Experimental relaxation spectra will be shown in section 3 to support the description of the evolution of the dynamics by the extended CM.

2.1. Coupling model for the fully cooperative relaxation at long times

The relevance of the CM to the dynamics of supercooled liquids is supported by

(1) the results of a specific example of the former to mimic several key experimentally observed properties of the latter [33] and
(2) the ability of its predictions to explain [34] the salient dynamic properties [14].

There is also a long history of application of the CM to explain key features of the ion dynamics in glassy, molten and crystalline ionic conductors [20, 24, 25, 28]. These examples, and in fact most previous applications of the CM, were focused on explaining the cooperative

motion of large amplitudes (of rotational angle or translational distance) at long times. For supercooled liquids, the latter is the structural α-relaxation or probe molecule relaxation. For ionic conductors, it is the cooperative ion hopping relaxation leading to dc conductivity. In these previous works, no consideration was given to the dynamics in the earlier-time regime when most of the relaxing units are caged. Naturally such caged dynamics involve motions with smaller amplitudes and no cooperativity, which will be further discussed in the next subsection. Thus, the only consideration given in previous works is that all relaxing units are no longer caged and ready to move independently to larger angles or distances, but such simultaneous independent relaxations are impossible because of the intermolecular (inter-ionic) interactions and constraints. Cooperativity is necessary for some successful motions of large amplitudes. Since all units are involved, we call this full cooperativity to distinguish it from a different scenario to be discussed in the next subsection. The independent relaxations of some units will not be successful in cooperative motions and the result is a slowed-down and dynamically heterogeneous relaxation process. The onset time of slowing down the independent relaxation, t_c, is of the order of 1 to 2 ps [31] for supercooled liquids and ionic conductors. The magnitude of t_c and its temperature independence reflects that the slowing down is caused by interaction. Rigorous solutions of simple models of an interacting system [32, 33] indicate that the independent relaxation, $\exp(-t/\tau_0)$, is slowed after t_c to a Kohlrausch–Williams–Watts (KWW) stretched exponential function [37, 38],

$$\phi(t) = \exp[-(t/\tau_K)^{1-n}]. \tag{1}$$

The coupling parameter, n, a positive fraction of unity, is a measure of the degree of slowing down. Operationally justified by the rather sharp crossover of the former to the latter as seen in model calculations [32, 33], a continuity between $\exp(-t/\tau_0)$ and the cooperative KWW relaxation function, equation (1), leads to the relation

$$\tau_K = [t_c^{-n}\tau_0]^{1/(1-n)}, \tag{2}$$

between the observed cooperative relaxation time, τ_K, and the independent relaxation time, τ_0. This relation together with the physical interpretation of n spawned many applications of the CM to several interacting systems with the benefit of explaining various phenomena and anomalous properties [25, 28, 34, 39, 40]. These long-time problems had been addressed successfully, notwithstanding the neglect of the caged dynamics at shorter time. In the next subsection, we extend the CM to include the contribution from caged dynamics.

2.2. Coupling model extended to include the short-time caged dynamics

Whether the long-time cooperative relaxation is the structural α-relaxation in supercooled liquids or the ion hopping relaxation in ionic conductors, it is the most prominent feature in the dielectric relaxation spectrum. From the fit of the KWW function or its Fourier transform to isothermal experimental data, the parameters, τ_K and n, are determined. With these parameters known, along with $t_c \approx 2$ ps [31], the independent relaxation time, τ_0, from equation (2) is given by

$$\tau_0 = t_c^n \tau_K^{1-n}. \tag{3}$$

Except at extremely high temperatures, initially at sufficient short times, all relaxing units are caged and vibrations are the only movements. However, the cages are not permanent because at any time there is non-zero probability for a unit to execute an independent relaxation. The probability is small in the early-time regime, $t \ll \tau_0$, because there is hardly any decay in the correlation function, $\exp(-t/\tau_0)$. Since the independent relaxations are rare and involve motions with small amplitudes, there is no cooperativity involved. The number of independent

relaxations increases with time throughout this early-time regime albeit very slowly, causing very slow decay of the cages or very slow increase of the mean square (angular or translational) displacement. In the frequency domain this corresponds to a loss which increases very slowly with decreasing frequency in the high-frequency regime defined by $\nu \ll \nu_0 \equiv 1/(2\pi\tau_0)$. The increase is so slow that it appears in the frequency spectrum as a nearly constant loss (NCL), extending over an extended range of frequencies. It is convenient to approximately describe the NCL by a power law, $\nu^{-\alpha}$, where α is a small positive number as often done in the literature of ionic conductors [15, 16, 22, 23]. It is important to remark here that a strict power law, $\nu^{-\alpha}$, is by no means necessary, but is only a convenient means to describe the slow increase of the loss.

As time continues to approach τ_0, there are an increasing number of independent relaxations due to a more significant decrease of $\exp(-t/\tau_0)$. Consequently there is a more rapid increase of the loss with decreasing frequency. NCL as defined by an approximate $\nu^{-\alpha}$-dependence for a chosen small positive α ceases to be observed below some frequency, $\nu_{x1} \equiv 1/(2\pi t_{x1})$, and we expect that $t_{x1} \ll \tau_0$ or $\nu_{x1} \gg \nu_0$.

At times comparable to τ_0, many units are independently relaxing and now some degree of cooperativity is required for motions to be possible. The degree of cooperativity continues to increase with time as more and more units participate in the motion. At some time, $t_{x2} \equiv 1/(2\pi\nu_{x2})$, after which the cages vanish, *all* units participate in the cooperative relaxation, and we have entered into the fully cooperative relaxation regime described by the original CM (previous subsection). It is clear that $t_{x2} \gg \tau_0$ or $\nu_{x2} \ll \nu_0$. These together with $t_{x1} \ll \tau_0$ or $\nu_{x1} \gg \nu_0$ demonstrate a pivotal role played by τ_0 (ν_0) in delineating three time (frequency) regimes of the dynamics. The *early*-time (higher-frequency) regime, $t < t_{x1}$ (or $\nu > \nu_{x1}$), exhibits the NCL. In the *intermediate*-time (frequency) regime, $t_{x1} < t < t_{x2}$ (or $\nu_{x1} > \nu > \nu_{x2}$), the probability of independent relaxations becomes significant and increases with time. Concomitantly, cooperativity is developing continuously with time in this intermediate-time regime. In the *long*-time (low-frequency) regime, $t > t_{x2}$ (or $\nu < \nu_{x2}$), full cooperativity has been developed and the time dependence is described by the KWW function (equation (1)). Naturally $t_{x2} < \tau$ (or $\nu_{x2} > \nu_K \equiv 1/2\pi\tau$). The characteristic times and frequencies introduced are related by

$$t_{x1} \ll \tau_0 \ll t_{x2} \ll \tau_K \tag{4}$$

and

$$\nu_{x1} \gg \nu_0 \gg \nu_{x2} \gg \nu_K. \tag{5}$$

From equation (2) it can be shown that

$$(\log\nu_0 - \log\nu_K) = n[\log\nu_c - \log\nu_K], \tag{6}$$

where $\nu_c \equiv 1/2\pi t_c$. Hence from equation (6), for the same ν_K, the separation between ν_0 and ν_K is smaller for a material having a smaller n. For the same material, the separation between ν_0 and ν_K becomes smaller at higher temperature, principally because of the increase of ν_K and also the possible decrease of n [33]. Thus, the width of the intermediate-time regime decreases with increasing temperature.

The above description of the spectrum could have been given qualitatively by any model which embodies the concept of a faster independent relaxation, as does the CM. However, what distinguishes the CM is that it offers a practical way to calculate the independent relaxation time or frequency, thus giving a quantitative underpinning, which can be evaluated against experimental data. Examples of such comparisons with experiment are given in the following sections for two classes of cooperatively relaxing systems, ionic conductors and supercooled liquids.

3. Dynamics of ions in glassy and molten ionic conductors

At sufficiently low frequencies, cooperative ion hopping makes the dominant contribution to the measurements given by the complex permittivity, $\varepsilon^*(\nu) = \varepsilon'(\nu) - \mathrm{i}\varepsilon''(\nu)$, or equivalently the complex conductivity, $\sigma^*(\nu) = \sigma'(\nu) + \mathrm{i}\sigma''(\nu) = \mathrm{i}2\pi\nu\varepsilon^*(\omega)$. Ion conductivity relaxation differs from dipole relaxation in supercooled liquids. Instead of measuring decay of polarization of dipoles in the latter, in the time domain, the measured electrical behaviour of the former can be described in terms of relaxation of the electric field, $E(t) = E(0)\phi(t)$, under the constraint of a constant displacement vector, D [41]. In the frequency domain, relaxation of polarization of permanent dipoles in non-conducting supercooled liquids is described by the dielectric permittivity, $\varepsilon^*(\nu)$, which is the electrical analogue of the complex mechanical compliance, $J^*(\nu)$, describing the response of the strain at constant stress. Electric field relaxation at constant D is then the electrical analogue of the complex mechanical modulus, $G^*(\nu)$, describing the response of the stress at constant strain. Hence for ionic motion, the most appropriate representation is not $\varepsilon^*(\nu)$ but the so-called complex electric modulus $M^*(\nu)$ [41]:

$$M^*(\nu) = M' + \mathrm{i}M'' = M_\infty\left[1 - \int_0^\infty \mathrm{d}t\ \exp(-\mathrm{i}2\pi\nu t)(-\mathrm{d}\phi/\mathrm{d}t)\right]. \tag{7}$$

$M^*(\nu)$ is related to $\varepsilon^*(\nu)$ by $\varepsilon^*(\nu) = 1/M^*(\nu)$, in analogy to $J^*(\nu) = 1/G^*(\nu)$. Let us consider first the part of the electric field decay and the corresponding part of the electric modulus, $M_n^*(\nu)$, caused by the fully cooperative movement of the ions. According to the original CM, $M_n^*(\omega)$ is obtained from equation (7) with $\phi(t)$ therein given by the Kohlrausch function (equation (1)). The corresponding dielectric loss, $\varepsilon_n^*(\nu) \equiv 1/M_n^*(\nu)$, and the conductivity, $\sigma_n^*(\nu) \equiv \mathrm{i}2\pi\nu/M_n^*(\nu)$, can also be obtained.

In the following sections we show that the interpretation of the evolution of ion dynamics by the extended CM is in accord with experimental data. There are many such examples, but only a few can be given in this work due to space limitation.

3.1. Ion dynamics of $0.4Ca(NO_3)_2$–$0.6KNO_3$ *(CKN) above* T_g

Shown in the inset of figure 1 are the $M''(\nu) \equiv \mathrm{Im}\, M^*(\nu)$ data of $0.4\mathrm{Ca(NO_3)_2}$–$0.6\mathrm{KNO_3}$ (CKN) at 342 K from [17, 18]. The glass transition temperature T_g is 333 K for CKN. The dashed line is the fit by $M_n''(\nu) \equiv \mathrm{Im}\, M_n^*(\nu)$ with $n = 0.34$. The main figure shows the data as $\varepsilon''(\nu)$ and the dashed line is $\mathrm{Im}\,\varepsilon_n^*(\nu)$. The data $\varepsilon''(\nu)$ deviate from $\mathrm{Im}\,\varepsilon_n^*(\nu)$ at higher frequencies and we determine ν_{x2} as the frequency above which the deviations are more than 10%. Similarly, we determine ν_{x1} as the frequency below which the data are more than 10% larger than the $\nu^{-\alpha}$-dependence chosen to represent the NCL. When data are not sufficient as in the present case, the ν_{x1} shown in figure 1 is somewhat arbitrary. Either from $\varepsilon''(\nu)$ or $M''(\nu)$, we can discern three spectral regimes discussed in the previous section:

(i) an NCL regime with $\alpha \approx 0$ for $\nu > \nu_{x1}$,
(ii) an intermediate crossover regime defined by $\nu_{x1} > \nu > \nu_{x2}$ and
(iii) the fully cooperative hopping regime for $\nu < \nu_{x2}$.

The location of the independent relaxation frequency, ν_0, calculated by equation (6) is indicated in the figure. The value of ν_c used in the calculation is 10^{11} Hz (or $t_c \approx 2$ ps), previously deduced from high-frequency/high-temperature measurements [31]. Note that a factor of two uncertainty in determining t_c or ν_c introduces via equation (6) uncertainty of only 2^n in ν_0, which is negligible for the present purpose. The most important point to make is that ν_0 lies well inside the intermediate-time regime and satisfies the inequality (5), which is necessary in order to justify the previously given interpretation of the spectrum by the extended CM.

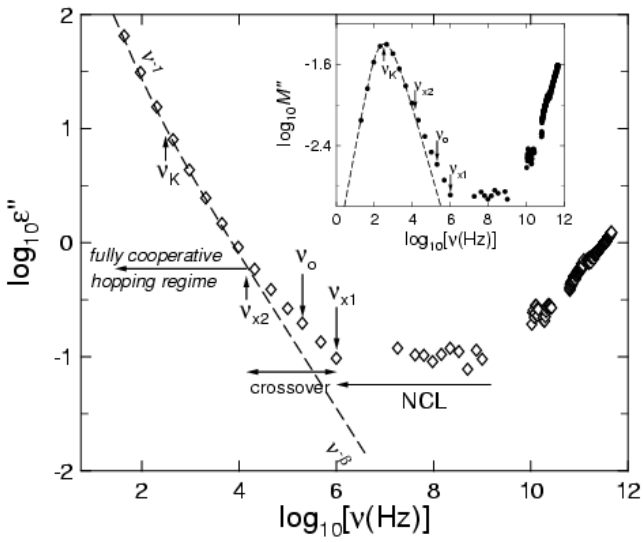

Figure 1. Dielectric loss ε'' as a function of frequency of CKN at 342.5 K showing the existence of the NCL over three decades in frequency. The dashed line is Im $\varepsilon_n^*(\nu)$ from the fully cooperative ion conductivity relaxation calculated from the Kohlrausch fit $M_n''(\nu) \equiv$ Im $M_n^*(\nu)$ to the electric loss modulus, M'', data shown in the inset as the dashed line with $n = 0.34$. The deviation of the data from the Kohlrausch fit at higher frequencies is marked by one crossover frequency, ν_{x2}. The deviation of the data from the NCL at lower frequencies is marked by the other crossover frequency, ν_{x1}. The locations of ν_K and the calculated independent relaxation frequency, ν_0, are also indicated. Data after [17] and [18].

Isothermal data similar to those shown for 342 K were produced by Lunkenheimer *et al* [17, 18] at 325.0, 350.3, 356.4, 361.0, 365.4, 370.0, 385.0, 393.0, 417.0, 440.0 and 468.0 K. Fits to these data in the electric modulus representation by $M_n^*(\nu)$ had previously been done by Lunkenheimer [18] and from his work the parameters n and ν_K are obtained for all temperatures. From these parameters ν_0 are calculated. Analyses of these data at other temperatures similar to that shown for 342 K give the parameters ν_{x1} and ν_{x2}, which define the frequency regimes for each temperature. In figure 2, ν_{x1}, ν_0, ν_{x2} and ν_K are plotted as functions of temperature. At all temperatures where all these four frequencies can be determined, inequality (5) is satisfied. The width of the transition zone is observed to decrease with increasing temperature, in agreement with the extended CM as discussed before, immediately following equation (6).

3.2. Ion dynamics in glassy $0.80LiF$–$0.20Al(PO_3)_3$

Electrical relaxation data of a glassy Li ion conductor, 0.80LiF–0.20Al$(PO_3)_3$, were obtained by Kulkarni *et al* [19] for many temperatures. In figure 3, we show their data in terms of $M''(\nu)$. An example of the Kohlrausch fit, $M_n''(\nu)$ with $n = 0.44$, is shown as the lone solid curve. The data represented as $\varepsilon''(\nu)$ are shown in figure 4 together with $\varepsilon_n''(\nu)$ calculated from the $M_n''(\nu)$ fits for two temperatures, 294.5 and 263.9 K (solid curves). The value of n does not depend on temperature in this glass. The experimental frequency range is not wide enough for the data at any temperature to show all three spectral regimes. Nevertheless, at low temperatures the NCL regime does appears in the experimental window (suggested by the line at the bottom with slope equal to -0.05), and at higher temperatures the fully cooperative regime appears as evidenced by $M_n''(\omega)$ or $\varepsilon_n''(\nu)$ fitting the data well. In figure 4, the arrows

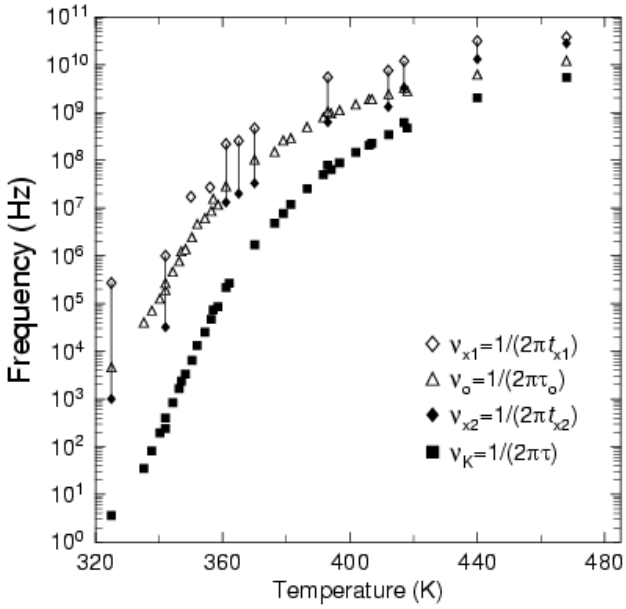

Figure 2. Solid squares are the Kohlrausch conductivity relaxation frequency ν_K obtained from the fits to the data of CKN [17, 18] at various temperatures in the electric modulus representation. Open triangles are ν_0 calculated from the fits. The open and closed diamonds are the crossover frequencies, ν_{x1} and ν_{x2}.

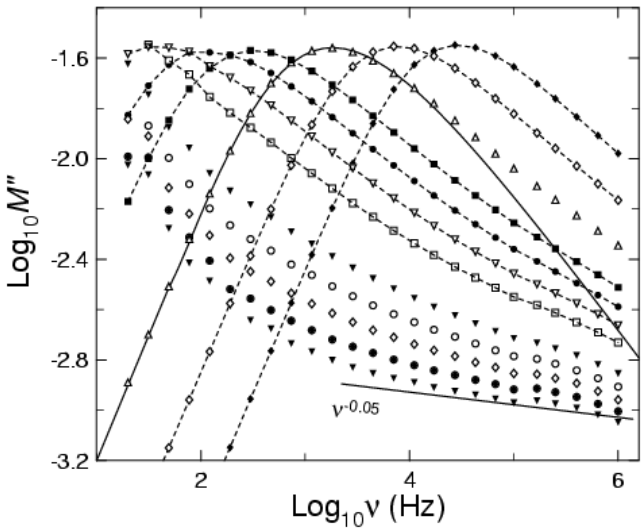

Figure 3. $\log_{10} M''(\nu)$ versus $\log_{10}\nu$ plot of data of 0.80LiF–0.20Al$(PO_3)_3$ obtained by Kulkarni *et al* [19]. From right to left, the data were taken at 335.2, 314.9, 294.5, 274.1, 263.9, 253.7, 243.5, 231.1, 212.9, 202.8, 192.4 and 182.5 K. The solid curve is the KWW fit $M_n''(\nu) \equiv \mathrm{Im}\, M_n^*(\nu)$ with $n = 0.44$ to the data at 294.5 K (△). The two dashed curves are used to guide the eyes. The solid straight line with slope −0.05 indicates the NCL.

pointing at the data at 263.9 K (filled circles) and the data at 294.5 K (open triangles) give the locations of ν_K and ν_0. Here ν_0 is calculated from equation (6) using $n = 0.44 \pm 0.02$,

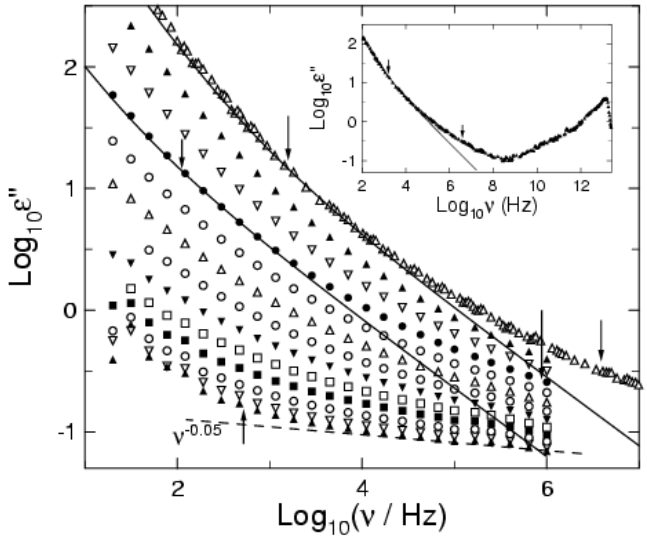

Figure 4. $\log_{10}\varepsilon''(\nu)$ versus $\log_{10}\nu$ plot of data of 0.80LiF–0.20Al$(PO_3)_3$ obtained by Kulkarni *et al* [19]. From top to bottom the data were taken at 294.5, 284.4, 274.1, 263.9, 253.7, 243.5, 233.3, 223.1, 212.9, 202.8, 192.4, 182.5 and 172.4 K. The solid curves are Im $\varepsilon_n^*(\nu)$ calculated for 294.5 (△) and 263.9 (●) from the KWW fits $M_n''(\nu) \equiv$ Im $M_n^*(\nu)$ to the electric modulus. The vertical arrows indicate ν_K and ν_0 for these two temperatures. The straight line with slope -0.05 indicates the NCL. The inset shows data of $\varepsilon''(\nu)$ at 294.5 K at higher frequencies to show that the NCL is responsible for the minimum.

and $\nu_c = 10^{11}$ Hz. In the glassy state, ν_K has Arrhenius temperature dependence [19]. By extrapolating the known Arrhenius temperature dependence down to 172.4 K, the lowest temperature of the data shown in figure 4, we determine ν_K and then calculate ν_0 again using $n = 0.44$, and $\nu_c = 10^{11}$ Hz. The arrow pointing towards the data (filled triangles) indicates the location of ν_0. The calculated ν_0 is significantly smaller than the frequencies where the NCL, operationally defined here by the $\nu^{-0.05}$-dependence, still holds. Thus, the condition, $\nu_{x1} \gg \nu_0$, for the lower bound of the NCL regime is again satisfied. In the inset the complete spectrum at 294.5 K is displayed. Now the extent of the NCL regime is compressed and is responsible for the minimum of $\varepsilon''(\nu)$. We can deduce by inspection of the inset that again the condition $\nu_{x1} \gg \nu_0$ holds. Such broadband dielectric measurement unfortunately has not been carried out at lower temperatures. Otherwise one could possibly see a more extended NCL regime in $\varepsilon''(\nu)$ at lower temperatures instead of a minimum at 294.5 K.

3.3. Ion dynamics in xK_2O–$(1-x)GeO_2$ glasses with $x = 0.02$

When ion concentration is low, interaction between ions is weak and the degree of cooperativity in the ion dynamics is small. Shown in figure 5 is such an example from $x\mathrm{K_2O}$–$(1-x)\mathrm{GeO_2}$ glasses with $x = 0.02$. The $\varepsilon''(\nu)$ data at 143.4 °C are taken from Jain and Krishnaswami [21]. These authors have already characterized the cooperative ion hopping by the Kohlrausch fit to the electric modulus data with $\beta \equiv (1-n) = 0.89$. The solid curve is the loss calculated from such a fit. The positions of ν_K from the fit and ν_0 calculated from equation (6) are indicated. The appearance of the NCL regime is clear. The two operationally determined crossover frequencies, ν_{x1} and ν_{x2}, are indicated in the figure. Again, ν_0 lies in between ν_{x1} and ν_{x2}, and inequality (5) is well satisfied. One may notice from figure 5 that the width of the

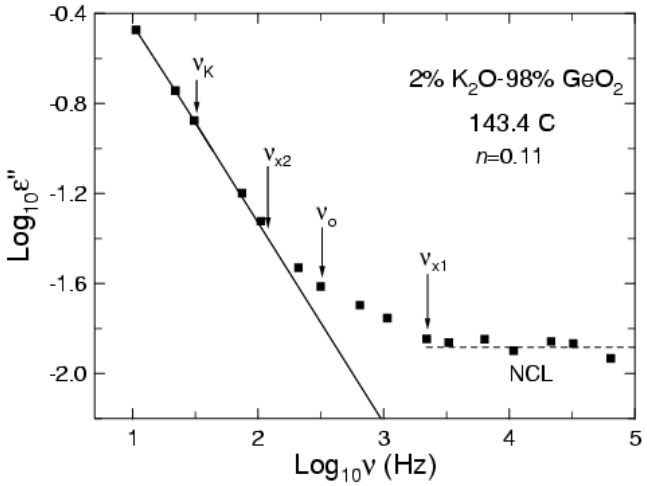

Figure 5. $\log_{10}\varepsilon''(\nu)$ versus $\log_{10}\nu$ plot of data of $x\mathrm{K_2O}$–$(1-x)\mathrm{GeO_2}$ glasses with $x = 0.20$ taken by Jain and Krishnaswami [21]. Here n is equal to 0.11 from a fit to the electric modulus (not shown) by Jain and Krishnaswami. The solid curve is Im $\varepsilon_n^*(\nu)$ calculated from the KWW fits to the electric modulus. The NCL regime appears at higher frequencies. The locations of ν_K and the calculated ν_0, as well as the crossover frequencies, ν_{x1} and ν_{x2}, are indicated by the vertical arrows.

intermediate regime of this glass is much narrower than that of $0.80\mathrm{LiF}$–$0.20\mathrm{Al(PO_3)_3}$ for a similar value of ν_K, in accordance with the extended CM as discussed immediately following equation (6).

4. Dynamics of supercooled molecular liquids

Long ago Johari and Goldstein (JG) showed the common occurrence of secondary or β-relaxation of *intermolecular* origin in supercooled liquids and glasses even for rigid molecules, which have no internal degrees of freedom [42–44]. Continued investigations by many other investigators have confirmed this view. Apparently the JG relaxation or process is a universal feature and an important aspect of the dynamics of supercooled glass-forming liquids. Various properties of the JG relaxation [12, 13] indicate that the process involves no cooperativity. Motivated by the fact that both the JG relaxations and the independent relaxation of the CM are non-cooperative processes in the same liquid, we have surmised that they may be closely related processes. In particular, it was proposed [13] that $\tau_0 \approx \tau_\beta$, or the corresponding frequencies, $\nu_0 = 1/(2\pi\tau_0)$ and $\nu_\beta = 1/(2\pi\tau_\beta)$, are about the same, i.e.,

$$\nu_0 \approx \nu_\beta. \tag{8}$$

In recent developments [13, 39, 45–47], by examining a large number of glass-formers, a close relation between the independent relaxation time of the CM, τ_0, and the most probable JG relaxation time, τ_β, has been established. This relation has been verified for many glass-formers at one temperature [13], namely T_g. Furthermore, equation (8) together with (6) (where ν_K therein is rewritten here as ν_α) implies that the distance between the α-peak and the JG β-peak, $\log\nu_\beta - \log\nu_\alpha$, is approximately given by

$$(\log\nu_\beta - \log\nu_\alpha) \approx (\log\nu_0 - \log\nu_\alpha) = n[\log\nu_c - \log\nu_\alpha]. \tag{9}$$

It is a decreasing function of the coupling parameter, n, in the KWW function, characterizing the deviation of the α-relaxation peak from the narrowest possible shape given by Debye. This is a remarkable prediction because it is made on the location of the JG relaxation but based on the coupling (nonexponentiality) parameter of the α-relaxation. For any fixed value of $\log \nu_\alpha$, a glass-former with smaller n has the JG relaxation located at $\log \nu_\beta$ that is closer to $\log \nu_\alpha$ of the α-relaxation peak, making the JG relaxation more difficult to be resolved. When n falls below some certain value, the JG relaxation can no longer be resolved within the spectral range of most experimental set-ups. In fact, experimentally most if not all glass-formers having smaller n values do not show a resolved JG relaxation [13] except by a special technique [3, 9]. The prediction given by equations (8) and (9) can be tested quantitatively by experimental data of glass-formers having resolved JG relaxation. So far the relation has been tested and verified in a large number of glass-formers but only at one temperature [13, 39, 45, 46], namely T_g, of each glass-former, except in a few cases [9, 47, 48]. This restriction is understandable because most dielectric relaxation measurements in the past have been limited to the more convenient frequency range of $1 < \nu < 10^6$ Hz. In this limited frequency range of at most six decades, it is not possible to see the resolved JG relaxation of glass-formers with larger n values at temperatures above T_g. For example, if $\nu_\alpha(T_g)$ is equal to 10^{-3} Hz, and n takes the medium value of 0.55, from equation (9) and $\nu_c \approx 10^{11}$ Hz (equivalent to $t_c \approx 2$ ps) we have $\nu_\beta(T_g) = 10^{4.7}$ Hz. At temperatures higher than T_g, ν_α is higher than 10^{-3} Hz and then ν_β is located outside the experimental frequency window. Thus JG relaxation is usually observed at temperatures significantly below T_g. Data that allow one to observe resolved JG relaxation at temperatures above T_g are rare. However, the latter if observed are challenging to test against the prediction of equation (8) for temperatures above T_g, as we consider next.

4.1. Glass-formers with resolved JG relaxation at temperatures above T_g

Only true JG relaxations are of interest to us to identify with the independent relaxation of the CM. Secondary relaxations originating from some decoupled internal degrees of freedom of the molecule are not JG relaxations. For various reasons that can be inferred from the chemical structures of the glass-formers or from the properties of the secondary relaxations themselves such as pressure dependence, the examples displayed in figures 6(a)–(f) are true JG relaxations. The sources of the dielectric relaxation data for 1, 4-polybutadiene [2, 46], sorbitol [6], 5-methyl-2-hexanol [8] and toluene [2] are published works. The data for xylitol [49] and BMMP (bis-methyl-methoxy-phenyl-cyclohexane) are new [50]. Since the resolved JG relaxation contributes to the dielectric loss on the high-frequency side of the α-relaxation peak, the criterion we use in fitting the KWW function to the α-relaxation peak is to emphasize good agreement with the data mainly at lower frequencies. Typical KWW fits to the loss data by ε_n'' from the one-sided Fourier transform,

$$\varepsilon_n'' = \Delta\varepsilon \,\mathrm{Im}\left[\int_0^\infty \mathrm{d}t \,\exp(-\mathrm{i}2\pi\nu t)(-\mathrm{d}\exp[-(t/\tau_K)^{1-n}/\mathrm{d}t)\right] \tag{10}$$

are shown by either the solid or dashed curves in figures 6(a)–(f). Some of these fits were carried out after removal of the small contribution to the loss at low frequencies from the dc conductivity, $\varepsilon_{dc}'' \propto \nu^{-1}$, but not shown in figures for the sake of clarity. From the fits to the isothermal data, we obtain ν_K and the coupling parameter n. For each glass-former, the selected data at temperatures not much above T_g were well fitted by a constant n, which is 0.56 ± 0.02 for 1, 4-polybutadiene (PBD), 0.52 ± 0.03 for sorbitol, 0.46 ± 0.02 for 5-methyl-2-hexanol, 0.46 ± 0.02 for xylitol, 0.44 ± 0.02 for toluene and 0.40 ± 0.02 for BMMPC,

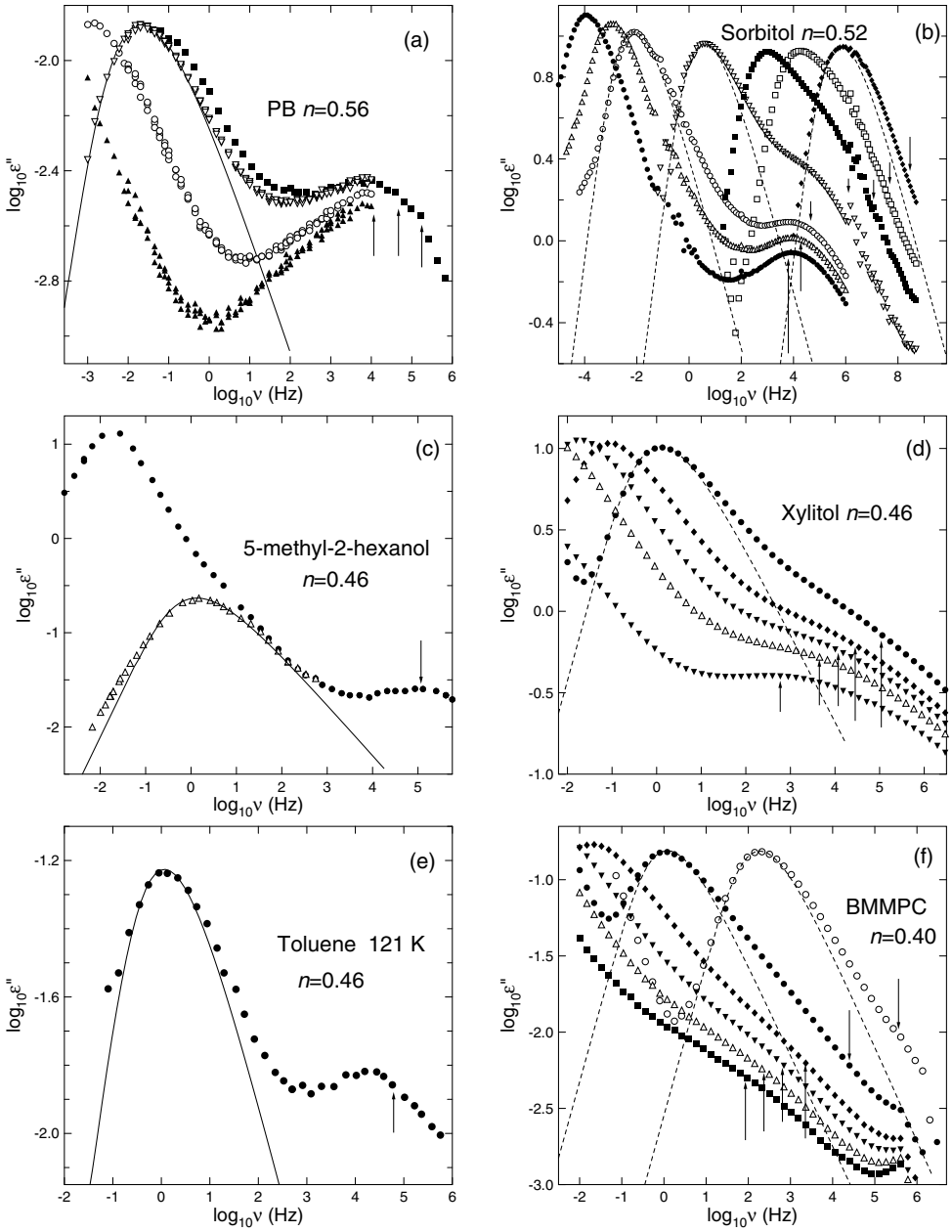

Figure 6. Isothermal dielectric loss data of six glass-formers that show resolved JG relaxation in the supercooled liquid state above T_g. Representative KWW fits to the α-relaxation peak are shown as curves. The value of n so determined is given in the figures. Each vertical arrow pointing towards certain data taken at a certain temperature indicates the location of the independent relaxation frequency, ν_0, calculated for that temperature. (a) 1, 4-polybutadiene data from [46] (▲, ○, ▽ at $T = -97.5$, -95, $-92.5\,^{\circ}$C respectively) and [2] (■ at -91.15 K). (b) Sorbitol data taken from [6] at 264, 266, 268, 276, 287, 296 and 312 K, from left to right. (c) 5-methyl-2-hexanol at $T = 158.2$ K from [8]. (d) Xylitol from [49] at 243, 248, 250, 252 and 254 K, from left to right. (e) Toluene from [2] at $T = 121$ K. (f) BMMPC from unpublished data [50] at several temperatures above T_g.

and they do not seem to depend on temperature when the α-relaxation peak frequencies fall below 10^2 Hz.

With n known, we can now calculate ν_0 by equation (9) at each temperature for the glass-formers, with the assumption that they all have the same $\nu_c = 10^{11}$ Hz, corresponding to $t_c \approx 2$ ps [31]. The location of each calculated ν_0 is indicated in the figures by a vertical arrow pointing at the data for which it applies, and it is also the location of the expected β-relaxation peak frequency, ν_β, if the identification between them can be made. The data in figures 6(a)–(f) show there are good correspondences between the calculated ν_0 and ν_β, and support the proposed close relation between the JG relaxation and the independent relaxation of the CM. The dielectric loss contributed by the independent relaxation in supercooled liquids is a peak (i.e. the JG relaxation peak) because decay of polarization from the dipole moment of the molecules is measured. On the other hand, in ionic conductors the independent relaxation contributes a monotonic increase of $\varepsilon''(\nu)$ with decreasing ν because the mean square displacement of ions is also a monotonic increasing function of time.

The spectral region in between ν_0 and ν_{x2} (below which the data is well fitted by the KWW function) is only part of the intermediate regime, $\nu_{x1} > \nu > \nu_{x2}$, of the extended CM. As explained before, various practical limitations of the experimental frequency window preempt the observation of both the NCL in the regime $\nu > \nu_{x1}$ and the JG relaxation at lower frequencies at temperatures above T_g. The spectra in figures 6(a)–(f) bear witness to this statement. Only at temperatures considerably below T_g, where even ν_0 or ν_β is moved amply outside the experimental frequency window, will one have the opportunity of seeing the NCL regime. This is demonstrated for xylitol in figure 6(d), where the data at the bottom taken below T_g at -173 K show an approximate $\nu^{-0.11}$ dependence over many decades. This weak frequency-dependent $\varepsilon''(\nu)$ could be considered as the high-frequency flank of an extremely broad β-relaxation peak of unknown origin. In the extended CM this is the NCL.

4.2. Glass-formers without resolved JG relaxation at temperatures above T_g

By inspection of figures 6(a)–(f), at constant ν_α or ν_K, one can see the separation between ν_α and ν_0 (or ν_β) is smaller in glass-formers with decreasing n. Among the six glass-formers in the figures, BMMPC has the smallest $n = 0.40$; the JG relaxation is closest to the α-relaxation and is barely resolved at temperatures above T_g. If the trend continues as expected from equation (9), glass-formers with smaller n will have the JG relaxation even closer to the α-relaxation such that they cannot be resolved. However, this encroachment of the JG relaxation towards the α-relaxation in glass-formers with smaller n opens up some spectral range for the observation of the NCL at temperatures near T_g. We explore this opportunity by examining dielectric relaxation data of some examples of such glass-formers.

Threitol [49] has $n = 0.36$, smaller than the coupling parameter of any of the glass-formers in figures 6(a)–(f), as shown by a representative KWW fit of ε''_n to the isothermal data in the inset of figure 7. The vertical arrows indicate the locations of ν_0 calculated for four temperatures, 232, 228, 226 and 224 K. Only at the two lowest temperatures 224 and 220 K near and slightly below T_g can the JG relaxation be barely resolved. The KWW exponent of the α-relaxation does not change with temperature near T_g. Thus by shifting the data at 232, 228 and 226 K horizontally to overlap the data at $T = 224$ K, an approximate master curve over nearly 12 decades is obtained for equilibrium liquid threitol and is shown in the main figure 7. Again the arrows indicate the locations of ν_0 calculated. The straight line with slope -0.13 is drawn merely to indicate the slow decrease of $\varepsilon''(\nu)$ with frequency.

On further decreasing n to 0.29 we have the case of glycerol. The isothermal data taken at $T = 179$, 185 and 190 K and shown in the inset of figure 8 were all obtained for glycerol

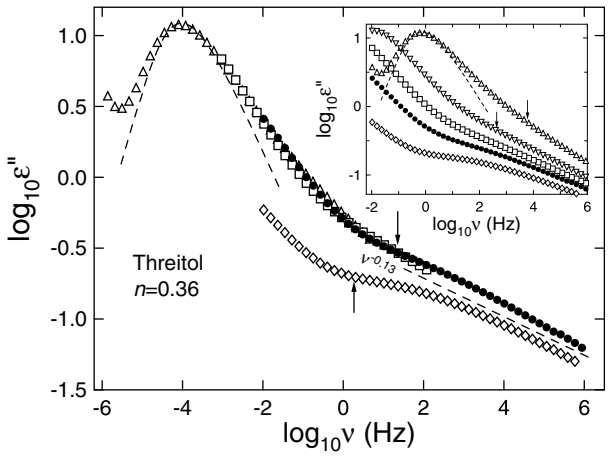

Figure 7. The inset shows the dielectric loss of threitol [49] at 220, 224, 226, 228 and 232 K, from left to right. The dashed curves are KWW fits to the α-relaxation peaks with $n = 0.36$. Each vertical arrow pointing towards certain data taken at some temperature indicates the location of the independent relaxation frequency, ν_0, calculated for that temperature. In the main figure the master curve obtained for $T = 224$ K (●) is shown (see text). The straight line with slope -0.13 is drawn to indicate the slow variation of ε'' at high frequencies.

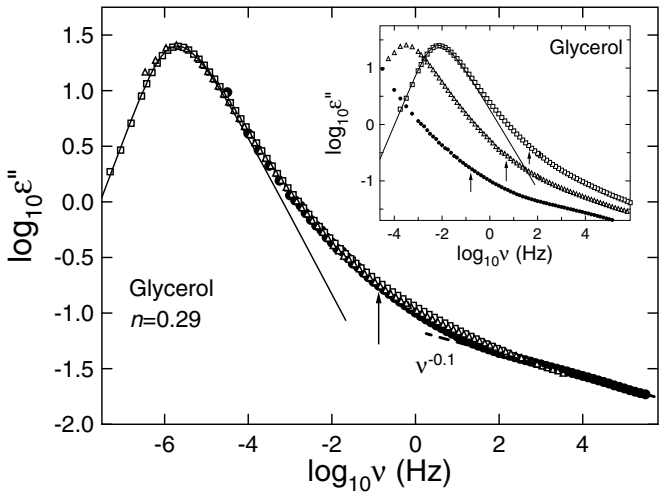

Figure 8. The inset shows the dielectric loss data of glycerol from [3] at three temperatures: 179 K, ●; 185 K, △, and 190 K, □. The data at 179 K were obtained after ageing to achieve thermodynamic equilibrium. The curve is fitted to the α-relaxation peak by the one-sided Fourier transform of the Kohlrausch function with $n = 0.29$. Each vertical arrow pointing towards certain data taken at some temperature indicates the location of the independent relaxation frequency, ν_0, calculated for that temperature. The main figure shows the master curve obtained by shifting the data at the two higher temperatures to superpose on the data at the lowest temperature 179 K (●). The vertical arrow indicates the location of the independent relaxation frequency, ν_0, calculated. The dashed line with frequency dependence, $\nu^{-0.1}$, indicates the slow variation of ε'' at high frequencies or the NCL regime.

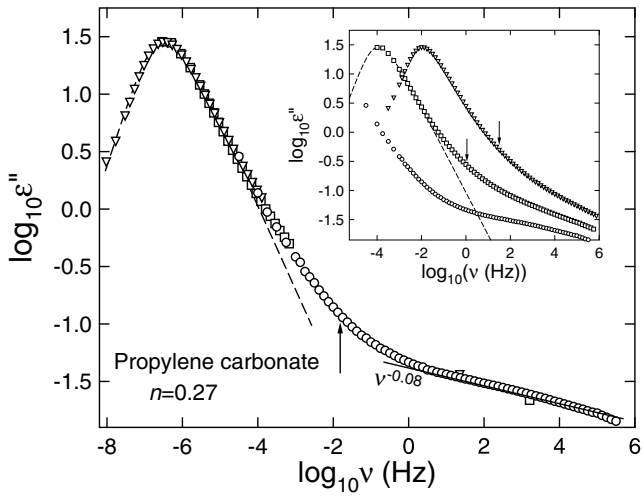

Figure 9. The inset shows the dielectric loss data of propylene carbonate from [3] at three temperatures: 152 K, ○; 155 K, □, and 158 K, ▽. The data at 152 K were obtained after ageing to achieve thermodynamic equilibrium. The curve is fitted to the α-relaxation peak by the one-sided Fourier transform of the Kohlrausch function with $n = 0.27$. Each vertical arrow pointing towards certain data taken at some temperature indicates the location of the independent relaxation frequency, ν_0, calculated for that temperature. The main figure shows the master curve obtained by shifting the data at the two higher temperatures to superpose on the data at the lowest temperature 152 K (○). The vertical arrow indicates the location of the independent relaxation frequency,ν_0, calculated. The dashed line with frequency dependence, $\nu^{-0.08}$, indicates the slow variation of ε'' at high frequencies or the NCL regime.

in the equilibrium liquid state by Schneider *et al* [3, 9]. At the lowest temperature of 179 K, equilibrium is achieved by ageing over several days, and the data exhibit an inflexion at the high-frequency wing, which indicates the presence of a JG relaxation [3]. The locations of the calculated ν_0 are indicated by the vertical arrows. The KWW exponent of the α-relaxation determined from the fits does not change with temperature near T_g. Thus by shifting the curves in the inset taken at $T = 185$ and 190 K horizontally to overlap the data at $T = 179$ K, an approximate master curve over nearly 14 decades is obtained for an equilibrium liquid glycerol and is shown in the main figure. From $\nu_\alpha = 10^{-5.7}$ Hz and $n = 0.29$ of the master curve, the expected β-relaxation peak frequency, ν_0, is calculated by equation (5) and its position is indicated by the lone vertical arrow. The decrease of $\varepsilon''(\nu)$ with frequency is very slow at high frequencies, approximately described by $\nu^{-0.1}$, as illustrated by the dashed line in the figure.

On further decreasing n, we have examples from propylene carbonate (PC), $n = 0.27$, and N-methyl-ε-caplolactam (NMEC), $n = 0.24$. In exactly the same manner as we did for glycerol, the isothermal data of PC [3] and NMEC [51] taken at equilibrium (insets in figures 9 and 10) are shifted to form master curves (figures 9 and 10). The PC data at the lowest temperature of 152 K were obtained [3] after ageing for days to achieve thermodynamic equilibrium.

The results of PC and NMEC in figures 9 and 10 all show similar frequency dispersion to glycerol, even though they have widely different molecular structures and are van der Waals liquids without hydrogen bonding. They all have NCL at high frequencies not much different from the approximate $\nu^{-0.1}$-dependence of glycerol. When temperature falls substantially below T_g, ν_K becomes so low that the entire α-relaxation peak, as well as ν_0, moves out of the experimental frequency window, and the NCL becomes the only observed feature in the

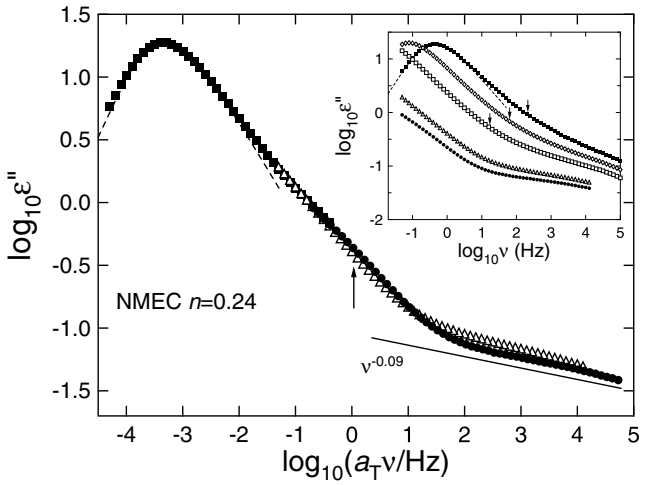

Figure 10. The inset shows the dielectric loss data of N-methyl-ε-caplolactam (NMEC) from [51] at several temperatures: 178 K, ■; 176 K, ◇; 174 K, □; 170 K, △, and 168 K, ●. The curve is fitted to the α-relaxation peak by the one-sided Fourier transform of the Kohlrausch function with $n = 0.25$. Each vertical arrow pointing towards certain data taken at some temperature indicates the location of the independent relaxation frequency, ν_0, calculated for that temperature. The main figure shows the master curve obtained by shifting the data at the other temperatures to superpose onto the data at 170 K (△).The vertical arrow indicates the location of the independent relaxation frequency, ν_0, calculated. The dashed line with frequency dependence, $\nu^{-0.09}$, indicates the slow variation of ε'' at high frequencies or the NCL regime.

dispersion as found experimentally [2, 52]. All these other glass-formers share the common characteristics of having smaller values of n, just like glycerol. Actually among these, glycerol has the largest n. The ratio of the NCL to the maximum loss of the α-peak seems to be about the same for two glass-formers having the same α-peak frequency ν_K.

Such a slow decrease of $\varepsilon''(\nu)$ with frequency of the NCL resembles the NCL found at high frequencies in glassy and molten ionic conductors discussed in section 2. The entire $\varepsilon''(\nu)$ dispersion of glycerol PC and NMEC shown in figures 8–10 bears some analogy to the ionic conductors. At high frequencies there is the NCL regime, defined by $\nu > \nu_{x1}$, with the upper bound ν_x satisfying the condition $\nu_0 \gg \nu_{x1}$. Then comes the intermediate-frequency regime, $\nu_{x1} > \nu > \nu_{x2}$, where $\varepsilon''(\nu)$ broadly crosses over from the NCL to a power law ν^{-n} at lower frequencies. Here n is the exponent in equation (1) for the KWW function that fits the data for $\nu < \nu_{x2}$. The upper bound of the intermediate-frequency regime or equivalently the lower bound of the KWW regime, ν_{x2}, satisfies the condition $\nu_{x2} \ll \nu_0$. The only difference in $\varepsilon''(\nu)$ between ionic conductors and dipolar supercooled liquids is at low frequencies. Ionic conductors have the ν^{-1}-dependence corresponding to dc conductivity of the mobile ions, while non-conducting dipolar liquids exhibit the α-loss peak. In glassy ionic conductors at sufficiently low temperatures when the cooperative ion hopping relaxation frequency ν_K as well as ν_0 becomes very low, the NCL is the only observed feature in the experimental frequency window [22], just like glycerol deep in the glassy state [2, 52]. These general properties found in ionic conductors have led to an interpretation of evolution of the dynamics of the ions from short times when they are caged to the long times when they are all engaged in slowed cooperative hopping motion [53, 54]. In the following subsection we shall give a similar interpretation to the molecular dynamics of glass-forming liquids.

4.3. Interpretation of the evolution of the molecular dynamics in supercooled liquids

A common practice in analysing dielectric loss data is to best fit the $\varepsilon''(\nu)$ to a superposition of the Fourier transform of the KWW function equation (10) (or a Cole–Davidson function) for the α-relaxation and a symmetric Cole–Cole function for the β-relaxation. The dispersion of the β-relaxation obtained from the fit is very broad at temperature near or below T_g. An example for glycerol at 185 and 179 K can be found in figure 1 of [9] and for PC at 152 and 155 K in figure 2 of the same reference, where such fits yield extremely broad distributions of β-relaxation frequencies. Although the existence of the β-relaxation in glycerol and PC is not in doubt because of the evidence provided by ageing [3, 9] and by the different response to pressure of the peak and the excess wing [55], it is not easy to understand why such extremely broad distributions of β-relaxation frequencies extending even below the most probable α-relaxation frequency, ν_K, can exist in an equilibrium liquid. In the following we shall give an alternative analysis and interpretation to the data in the equilibrium liquid state.

We start with the 'master' spectra of glass-formers shown in the main parts of figures 8–10. The crux of the interpretation is the independent relaxation frequency, ν_0, we have calculated by equation (9) from the parameters, ν_K and n, of the α-peak obtained in fitting it to the KWW function. In all cases, ν_0 is located between the KWW α-peak and the NCL regime at high frequencies. Specifically ν_0 is about two decades higher than the frequency, ν_{x2}, below which the Fourier transform of the KWW function accurately describes the α-peak. Also ν_0 is about two decades lower than the frequency, ν_{x1}, above which the NCL regime takes hold. The interval, $\nu_{x2} < \nu < \nu_{x1}$, is appropriately called the transition zone separating the NCL regime ($\nu_{x1} < \nu$) from the KWW regime ($\nu < \nu_{x2}$). Since ν_0 is the independent relaxation or reorientation time of a molecule, the fact that $\nu_0 \ll \nu_{x1}$ implies the probability of such independent reorientations, given by $[1 - \exp(-t/\tau_0)] = [1 - \exp(-\nu_0/\nu)]$, is small when $\nu > \nu_{x1}$. Hence few independent reorientations occur in the NCL regime and this explains the low dielectric loss and the very slow increase with frequency of ε'' in the NCL regime (see figures 8–10). Thus in the NCL regime, most molecules are still 'caged', meaning that they have not made the independent reorientation to get themselves out of the cages. The small NCL in this caged period is nevertheless contributed to by the independent reorientations of a few. As frequency is decreased (or time is increased), the probability of such independent reorientations monotonically increases and there will be a time (frequency ν_{x1}) beyond which the dependence of ε'' no longer fits into the definition of NCL (i.e., say 10% deviation from the approximate power law $\nu^{-\alpha}$). The deviation of ε'' from the NCL increases on further decrease of frequency below ν_{x1}, because of the monotonically increasing probability of independent reorientations. When the frequency is comparable to ν_0, the probability of independent reorientations becomes significant, giving rise to the JG peak at frequency $\nu_\beta \approx \nu_0$. At frequencies further below ν_0, many more molecules are now attempting to make independent orientations, but not all of them are successful because of the omnipresent interaction/coupling between molecules. Some degree of cooperativity has to be involved, where cooperativity is used here in the sense that attempts of some molecules to reorient are unsuccessful in order to make possible successful attempts of other molecules. Thus cooperativity entails dynamic heterogeneity. The degree of cooperativity increases with decreasing frequency because of the increasing number of molecules making such attempts. When ν falls sufficiently below ν_0, all molecules have practically a 100% probability of attempting independent reorientations, and the regime of fully cooperative dynamics with the KWW correlation function is reached and prevails thereafter. This scenario, that none of the molecules (or basic units in the more general context of the CM) is caged and all are ready to execute the independent relaxations but are preempted by interactions/coupling, is assumed to be the case in all previous theoretical considerations

[30–34] and applications of the CM to the α-relaxation (or whichever ultimate relaxation process of the basic units in other systems). In other words, no consideration has been given to the earlier stages of the dynamics when essentially most of the molecules are still caged (i.e., the NCL regime) and the gradual development of cooperativity when increasing numbers of molecules are ready to reorient independently (i.e., the transition zone). Here, for the first time, we include the dynamics of earlier times and a more complete description of the CM results. From the original CM [30–33] the fully cooperative dynamics corresponds to ε^* being well described by the Fourier transform of the KWW function. Thus ν_{x2} as defined earlier is the frequency for onset of fully cooperative dynamics. The slowing down of the independent reorientations in the fully cooperative dynamics is caused by the interaction/coupling between the molecules, starting out from a temperature-independent time, t_c. Equation (2) (or the equivalent equations (6) and (9)) is a consequence of such onset, and has been instrumental in locating the independent reorientation frequency, ν_0, from the parameters, n and τ_α, of the KWW fit to the α-relaxation. The above description of the evolution of the molecular dynamics of glass-formers supported by experimental data would not be credible unless the independent reorientation frequency were given quantitatively and its location were consistent with the interpretation. The CM enables ν_0 to be calculated and its location is consistent with the JG peak frequency ν_β, and the interpretation of the origins of the NCL and the transition zone (figures 6–10). The broad width of the JG relaxation is accounted for by the broad transition from the NCL to the fully cooperative KWW relaxation. The relaxation strength of the JG relaxation can be inferred from that of the independent relaxation. The only difference between the independent relaxation and the α-relaxation is the slowing down of its relaxation time from τ_0 to τ_α or τ_K due to intermolecular coupling (equation (6)). Other than this difference, the independent relaxation has the same dependence on specific volume or configurational entropy as the α-relaxation. Hence, from our identification of the JG relaxation with the independent relaxation, the temperature dependence of the dielectric strength of the JG relaxation will reflect that of the structural relaxation across T_g, as observed [56, 57].

The description we give here for the evolution of the molecular dynamics as a function of time/frequency for supercooled liquids is analogous to that given earlier for the ion dynamics in ionic conductors. This similarity is supported by the experimental data presented and is in accord with the view of the CM that some fundamental physics govern the relaxation dynamics of interacting systems, giving rise to generic properties. This view has support from the observation by dynamic light scattering of the NCL in polyisobutylene, a polymeric glass-former, and other substances [58, 59]. We have pointed out elsewhere [53] that data from the time domain confocal microscopy of colloidal supercooled liquids [26, 27] also exhibit the three regimes of NCL, the transition zone and the fully cooperative regime. From molecular dynamics simulation data of ion dynamics in a glassy ionic conductor [53] we have demonstrated that the temporal development of the self-part of the van Hove function supports the interpretation given here. The time dependence of the non-Gaussian parameter calculated from the molecular dynamics data of the glassy ionic conductor strongly resembles that of the supercooled colloidal particles [26, 27] and binary Lennard-Jones liquids from simulation [60]. All these facts provide additional evidence for a common description of the relaxation dynamics of cooperatively relaxing systems and support for the interpretation based on the extended CM given here.

5. Conclusion

From analyses of experimental data by using the concept of independent relaxation of the CM and its relaxation time that can be obtained quantitatively, we have arrived at a description of the

evolution with time of the ion dynamics in glassy or molten ionic conductors and molecular reorientation relaxation in supercooled liquids. The evolution can be roughly divided into three principal time/frequency regimes: the NCL at high frequencies, a transition zone at intermediate frequencies and the fully cooperative ion hopping or molecular reorientation regime at low frequencies. It is remarkable that a common description of the dynamics is shared by two different cooperatively relaxing systems: ion hopping dynamics in ionic conductors involving translations of 'point' charged particles, and dynamics in supercooled liquids involving reorientation of densely packed molecules. The crux of the extended CM interpretation is the calculated independent relaxation time/frequency. Its position within the transition zone enables the physical interpretation of the NCL, and its interpretation as being the precursor of the cooperative structural α-relaxation. From dielectric spectra of the supercooled liquids exhibiting resolved JG relaxation, we find that the most probable JG β-relaxation frequency is nearly the same as this calculated independent relaxation frequency. Hence the JG β-relaxation, commonly considered to be a universal feature of glass-formers, provides evidence of the same for the independent relaxation in the extended CM.

Acknowledgments

This work was supported by the Office of Naval Research. I thank the following colleagues for generously providing experimental data: A Kulkarni for $0.80LiF–0.20Al(PO_3)_3$, P Lunkenheimer and A Loidl for glycerol and propylene carbonate, R Nozaki for sorbitol, M Paluch for BMMPC and R Richert for NMEC. I also thank R Casalini, J Habasaki, C León, P Lunkenheimer and M Paluch for collaborations, and C M Roland for a critical reading of the manuscript.

References

[1] Wagner H and Richert R 1998 *J. Non-Cryst. Solids* **242** 19
[2] Wiedersich J, Blochowicz T, Benkhof S, Kudlik A, Surovtsev N V, Tschirwitz C, Novikov V N and Rössler E 1999 *J. Phys.: Condens. Matter* **11** A147
Kudlik A, Tschirwitz C, Blochowicz T, Benkhof S and Rössler E 1999 *J. Non-Cryst. Solids* **235–237** 406
[3] Schneider U, Brand R, Lunkenheimer P and Loidl A 2000 *Phys. Rev. Lett.* **84** 5560
[4] Schönhals A 2001 *Europhys. Lett.* **56** 815
[5] Andreozzi L, Faetti M, Giandano M and Leporini D 1999 *J. Phys.: Condens. Matter* **11** A131
[6] Nozaki R, Suzuki D, Ozawa S and Shiozaki Y 1998 *J. Non-Cryst. Solids* **235–237** 393
[7] León C, Ngai K L and Roland C M 1999 *J. Chem. Phys.* **110** 11585
[8] Kalinovskaya O E and Vij J K 2000 *J. Chem. Phys.* **112** 3262
[9] Ngai K L, Lunkenheimer P, León C, Schneider U, Brand R and Loidl A 2001 *J. Chem. Phys.* **115** 1405
[10] Paluch M, Ngai K L and Hensel-Bielowka S 2001 *J. Chem. Phys.* **114** 10872
[11] Döß A, Paluch M, Sillescu H and Hinze G 2002 *Phys. Rev. Lett.* **88** 95701
[12] Vogel M and Rössler E 2000 *J. Phys. Chem.* B **104** 4285
[13] Ngai K L 1998 *J. Chem. Phys.* **109** 6982
[14] Ngai K L 2000 *J. Non-Cryst. Solids* **275** 7
[15] Burns A, Chryssikos G D, Tombari E, Cole R H and Risen W M 1989 *Phys. Chem. Glasses* **30** 264
[16] Angell C A 1990 *Chem. Rev.* **90** 523
[17] Lunkenheimer P, Pimenov A and Loidl A 1997 *Phys. Rev. Lett.* **78** 2995
[18] Lunkenheimer P 1999 *Dielectric Spectroscopy of Glassy Dynamics* (Aachen: Shaker)
[19] Kulkarni A, Lunkenheimer P and Loidl A 1999 *Ceramics Trans.* **92** 115
[20] Ngai K L and Moynihan C T 1998 *Bull. Mater. Res. Soc.* **23** 51
[21] Jain H and Krishnaswami S 1998 *Solid State Ion.* **105** 129
[22] León C, Rivera A, Várez A, Sanz J, Santamaría J and Ngai K L 2001 *Phys. Rev. Lett.* **86** 1279
[23] Ngai K L 1999 *J. Chem. Phys.* **110** 10576
[24] Ngai K L, Greaves G N and Moynihan C T 1998 *Phys. Rev. Lett.* **80** 1018

[25] Ngai K L 1998 *Phil. Mag.* **77** 187
[26] Weeks E R, Crocker J C, Levitt A, Schofield A and Weitz D A 2000 *Science* **287** 627
[27] Weeks E R and Weitz D A 2002 *Phys. Rev. Lett.* **89** 095704
[28] Ngai K L 1994 *Disorder Effects on Relaxational Properties* ed R Richert and A Blumen (Berlin: Springer) pp 89–150
[29] Götze W 1999 *J. Phys.: Condens. Matter* **11** A1
[30] Ngai K L 1979 *Comments Solid State Phys.* **9** 121
[31] Ngai K L and Rendell R W 1997 *Supercooled Liquids, Advances and Novel Applications (ACS Symp. Series vol 676)* ed J T Fourkas *et al* (Washington, DC: American Chemical Society) p 45
[32] Tsang K Y and Ngai K L 1996 *Phys. Rev.* E **54** R3067
Tsang K Y and Ngai K L 1997 *Phys. Rev.* E **56** R17
[33] Ngai K L and Tsang K Y 1999 *Phys. Rev.* E **60** 4511
[34] Ngai K L 2001 *IEEE Trans. Dielectr. Electr. Insul.* **8** 329
[35] Cummins H Z, Li G, Hwang Y H, Shen G Q, Du W M, Hernadea J and Tao N J 1997 *Z. Phys.* B **103** 501
[36] Schneider U, Brand R, Lunkenheimer P and Loidl A 1999 *Phys. Rev.* E **59** 6924
[37] Kohlrausch R 1847 *Pogg. Ann. Phys.* **12** 393
[38] Williams G and Watts D C 1970 *Trans. Faraday Soc.* **66** 80
[39] Ngai K L 1999 *J. Phys.: Condens. Matter* **11** A119
[40] Ngai K L 2002 *Eur. Phys. J.* E **8** 225
[41] Moynihan C T 1994 *J. Non-Cryst. Solids* **172–174** 1395
Moynihan C T 1996 *J. Non-Cryst. Solids* **203** 359
Moynihan C T 1998 *Solid State Ion.* **105** 75
[42] Johari G P and Goldstein M 1970 *J. Chem. Phys.* **53** 2372
[43] Johari G P 1973 *J. Chem. Phys.* **58** 1766
[44] Johari G P 1976 *Ann. NY Acad. Sci.* **279** 117
[45] Ngai K L 1999 *Macromolecules* **32** 7140
[46] Casalini R, Ngai K L, Robertson C G and Roland C M 2001 *J. Polym. Sci. Polym. Phys. Edn* **38** 1841
[47] Ngai K L and Roland C M 2002 *Polymer* **43** 567
[48] Rault J 1999 *J. Non-Cryst. Solids* **260** 164
[49] Ngai K L and Paluch M 2002 *J. Phys. Chem.* B submitted
[50] Paluch M Unpublished data
[51] Schüller J, Richert R and Fischer E W 1995 *Phys. Rev.* B **52** 15232
[52] Hoffmann A, Kremer F, Fischer E W and Schönhals A 1994 *Disorder Effects on Relaxational Processes* ed R Richert and A Blumen (Berlin: Springer)
[53] Habasaki J, Ngai K L and Hiwatari Y 2002 *Phys. Rev.* E **66** 021205
[54] Ngai K L and León C 2002 *Phys. Rev.* B **66** 064308
[55] Paluch M, Casalini R, Hensel-Bielowka S and Roland C M 2002 *J. Chem. Phys.* **116** 9839
[56] Yagihara S, Yamada M, Asano M, Kanai Y, Shinyashiki N, Mashimo S and Ngai K L 1998 *J. Non-Cryst. Solids* **235–237** 809
[57] Johari G P, Power G and Vij J K 2002 *J. Chem. Phys.* **116** 5908
[58] Sokolov A P, Kisluik A, Novikov V N and Ngai K L 2001 *Phys. Rev.* B **63** 172204
[59] Caliskan G, Kisluik A, Sokolov A P and Novikov V N 2001 *J. Chem. Phys.* **114** 10189
[60] Kob W, Donati C, Plimton S J, Poole P H and Glotzer S C 1997 *Phys. Rev. Lett.* **79** 2827